Indian Journal of Chemistry
Vol. 56A, May 2017, pp. 493-500

Poly(*o*-toluidine) salt as low cost electrode material for high performance electrochemical supercapacitor

Hajera Gul[a], Salma Gul[a, b], Anwar-ul-Haq Ali Shah[c] & Salma Bilal[a, *]

National Center of Excellence in Physical Chemistry, University of Peshawar, Pakistan

Email: salmabilal@uop.edu.pk

[b]Women University Swabi, 22102 Swabi, Pakistan

[c]Institute of Chemical Sciences, University of Peshawar, 25120 Peshawar, Pakistan

Received 18 January 2017; revised and accepted 19 April 2017

Binder-free, low cost poly(*o*-toluidine) (POT) has been synthesized by emulsion polymerization method. The synthesized POT salt has been tested for supercapacitor application through cyclic voltammetry and galvanostatic charge discharge analysis. The POT salt exhibits a specific capacitance value of 301 F/g. The synthesized material was further characterized by FTIR, UV-visible spectroscopy and X-ray diffraction analysis.

Keywords: Electrochemistry, Electrodes, Cyclic voltammetry, Galvanostatic charge discharge, Poly(*o*-toluidine)

Environmental changes and the hampered accessibility of fossil fuels have enormously influenced the ecology and world economy[1]. With the improvement in hybrid electric vehicles and fast growth of the business sector for movable electronic devices, there has been increasing and vital interest for ecofriendly high-power energy resources[2]. Supercapacitors (SC) have gained much consideration due to their long cyclic life, simple principle, high dynamic of charge propagation and pulse power supply[3, 4]. At present, semiconductors are broadly utilized as a parts of customer gadgets, memory back-up systems, industrial power and energy management[1].

There are two fundamental types of the capacitance of SC, based on their charge storage mechanism[5, 6]: (i) electrical double layer capacitance which originates from charge partition at electrode/electrolyte interface[7] and is controlled by the dielectric constant of the electrolyte and effective surface area, and, (ii) pseudocapacitance due to fast faradic reactions of the electrode material[8]. Double-layer capacitance originates from a surface process, while pseudocapacitance originates from a bulk process[9]. Materials which are used to build semiconductors are mainly the materials based on carbon (including carbon aero-gel, active carbon and carbon nanotube), metal oxides (RuO_2, IrO_2 and MnO_2) and electrically conducting polymers (including polyaniline (PANI), polypyrrole, and polythiophene)[10].

The reversible faradic responses of electrically conducting polymers (ECPs) together with doping/dedoping of dopants create high pseudocapacitance[11]. In this regard, PANI is considered as the most important material because of its high capacitance and conductivity[12]. PANI is frequently studied for supercapacitors. However, its practical utilization has been restricted by its insolubility in organic solvents because of the delocalized π bonds along their backbone[13]. Due to improved processability, substituted derivatives of polyanilines have been utilized for numerous applications[10].

Poly(*o*-toluidine) (POT), the polymer synthesized from *o*-toluidine (OT) (substituted aniline with a $-CH_3$ on the *ortho* position in aromatic ring)[14], has been shown to display redox behavior and structural properties very closely related to those of PANI. Among all four oxidation states, emeraldine salt is the only conducting form of POT[15].

In this study, we explore the use of POT-salt as binder-free, low cost material for energy storage applications in SC as the introduction of a binder into the electrode results in reduction of the overall conductivity of the electrode and hence power density[16]. The various properties of the synthesized POT-salt were further investigated through different techniques, such as UV-visible spectroscopy and X-ray diffraction analysis. To the best of our knowledge there is no literature available on the use of POT-salt in supercapacitors applications.

Experimental

Research grade reagents were used throughout the experimental work. *o*-Toluidine (OT, Acros) was distilled. Dodecylbenzenesulfonic Acid (DBSA) and acetone were purchased from Acros, while chloroform, sulfuric acid (H_2SO_4) and ammonium persulfate, $(NH_4)_2S_2O_8$ from Riede-de Haen and were used as such.

POT salt was prepared by chemical oxidative polymerization method reported earlier[17]. In a typical experiment, 50 mL chloroform was taken in a 100 mL round bottom flask and 2.3 mL DBSA was added to it under mechanical stirring. *o*-Toluidine (1.5 mL) and 25 mL of 0.5 *M* H_2SO_4 were added to the above solution. Then 25 mL of 0.05 *M* ammonium persulfate was added to the resulting mixture. The mixture turned green and the polymerization reaction was allowed to proceed for 24 h. Finally, the organic phase containing POT salt was separated and washed four times with 50 mL acetone. After thorough washing, a dark green, highly concentrated POT salt was obtained. It was dried at room temperature for 24 hours in a petri dish. On addition of a small amount of acetone to the petri dish, the film broke into flakes to yield the POT salt which was separated by filtration and dried in a desiccator.

By varying the concentration of H_2SO_4, the experimental conditions were optimized. The polymers obtained with different concentrations of H_2SO_4 were labeled as POT-1, POT-2, POT-3, POT-4 and POT-5 where H_2SO_4 concentrations were 0.3 *M*, 0.5 *M*, 0.9 *M*, 1.3 *M* and 1.7 *M*, respectively.

Cyclic voltammetry (CV) and galvanostatics charge discharge analysis (GCD) of the POT salts were executed in a three-electrode electrochemical cell using a 3000 ZRA potentiostat/galvanostat (Gamry, USA). The POT salt dip coated onto the surface of gold sheet was used as the working electrode, while a coiled wire of gold and saturated calomel electrode (SCE) were used as counter electrode and as reference electrode, respectively with 2 *M* H_2SO_4 as electrolyte. Ultraviolet visible (UV-vis) spectroscopic analysis was carried out in chloroform using a Perkin Elmer spectrophotometer having a quartz cell of 1 cm path length. Structural analysis of POT salt was done by Fourier transform infrared (FTIR) spectroscopy (Shimadzu, Japan) in the 400-4000 cm^{-1} range. The X-ray diffraction analysis of PANI samples were carried out at room temperature with a Rigaku X-Ray diffractometer (Japan).

Results and discussion

Cyclic voltammograms (CVs) of POT salts recorded at different scan rates are depicted in Fig. 1. The CV displays two couples of redox peaks indicating pseudocapacitance phenomenon[18]. The first anodic peak is due to the conversation of leucoemeraldine form of POT to the emeraldine state, while the second peak is because of the transformation of emeraldine to pernigraniline[15, 19, 20]. Any intermediate peak between the first and second oxidation peaks is absent in the CVs of all samples recorded at different scan rates, which indicates that no degradation products are formed[21]. As

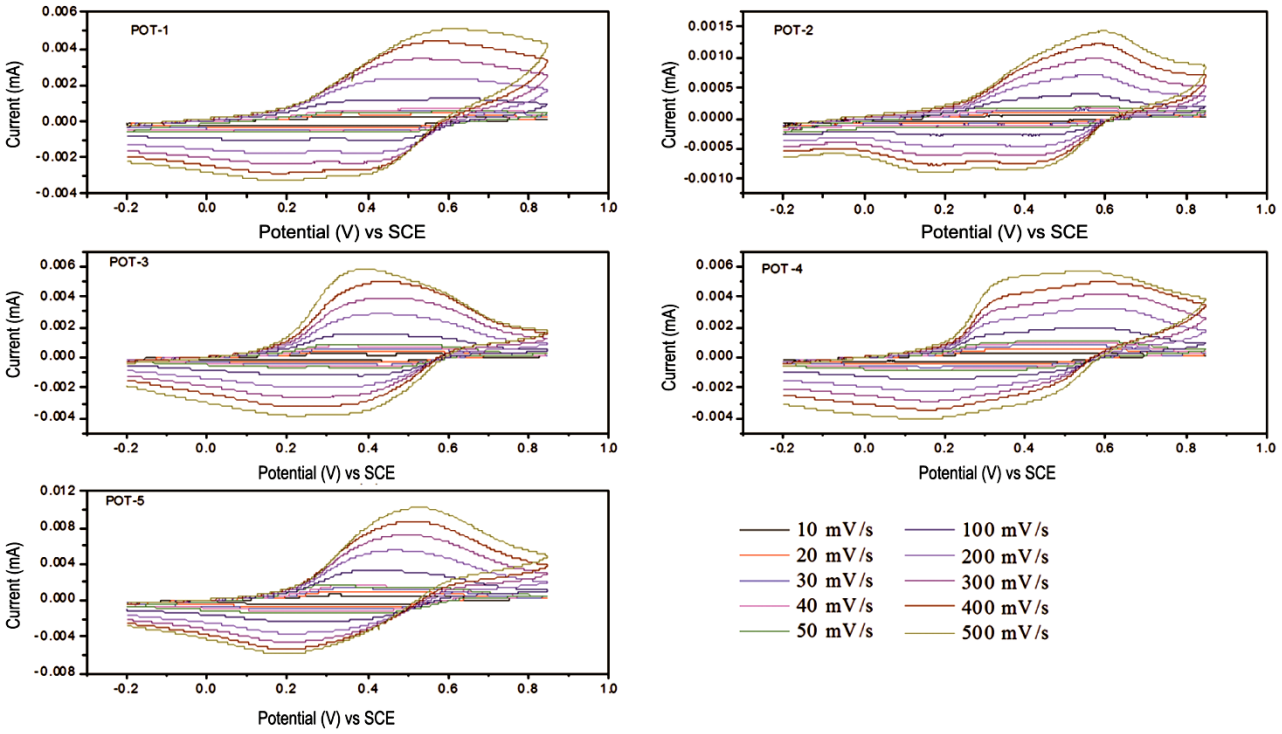

Fig. 1 — CVs of POT-1, POT-2, POT-3, POT-4 and POT-5 at varying scan rate (10-500 mV/s) versus SCE in 2 *M* H_2SO_4.

shown in Fig. 2a, the CV current increases linearly with an increase in the scan rate, which signifies highly stable supercapacitive characteristics of the POT-salts[22]. The synthesized polymer shows outstanding electrochemical behavior in a broad range of scan rates (10, 20, 30, 40, 50, 100, 200, 300, 400 and 500 mV/s). It was observed that the oxidation peaks moved positively and reduction peaks negatively with rising scan rates, which is due to resistance of the electrode. Moreover, the peak currents increase linearly with square root of the scan rate, revealing diffusion limited redox process (Fig. 2a)[23]. The distinct enhancement of peak current with increasing scan rate is indicative of good performance of the synthesized material[22]. Specific capacitance was calculated at different scan rate by using formula, $C = i/\upsilon \times m$, where "i" is the maximum peak current, "v" is the scan rate and "m" is the mass of the deposited material. It is shown that with increasing scan rate, the specific capacitance value decreases (Fig. 2b). This decline in specific capacitance value with increasing sweep rate may be due to the presence of internal active sites which cannot sustain the redox transition perfectly at higher scan rates[24]. In Fig. 2b, the overall specific capacitance value increases from POT-1 to POT-5. The POT-5 shows a maximum value of 311 F/g. This increase in specific capacitance value from POT-1 to POT-5 can be ascribed to the increasing doping level with DBSA. Insertion of higher amount of DBSA in POT increases the extent of conjugation length. Electrochemical properties seem to be enhanced because of interaction between POT backbone and DBSA alkyl chain[25]. This increase in doping level was also confirmed by UV-visible, FTIR and XRD data *vide infra*.

Mechanism of charging/discharging in POT-salt can be readily explained by CV data. As discussed above, cyclic voltammogram of POT presents two main redox peaks corresponding to the interconversion of three oxidation states, i.e., leucoemeraldine, emeraldine salt and pernigraniline. The process consists of insertion and elimination of anions from POT chain which results in charging and discharging of the electrode material. It has been reported[26] that during charging of the capacitor, POT in emeraldine salt either transform to pernigraniline or leucoemeraldine by elimination of the anions. During discharging, POT converts from pernigraniline or leucoemeraldine to emeraldine salt form by insertion of anion into the polymer chain as shown in Scheme 1.

Electrochemical performance of POT-salt was further explored through galvanostatic charge-discharge analysis at two different tested currents. The galvanostatic charge-discharge study of POT

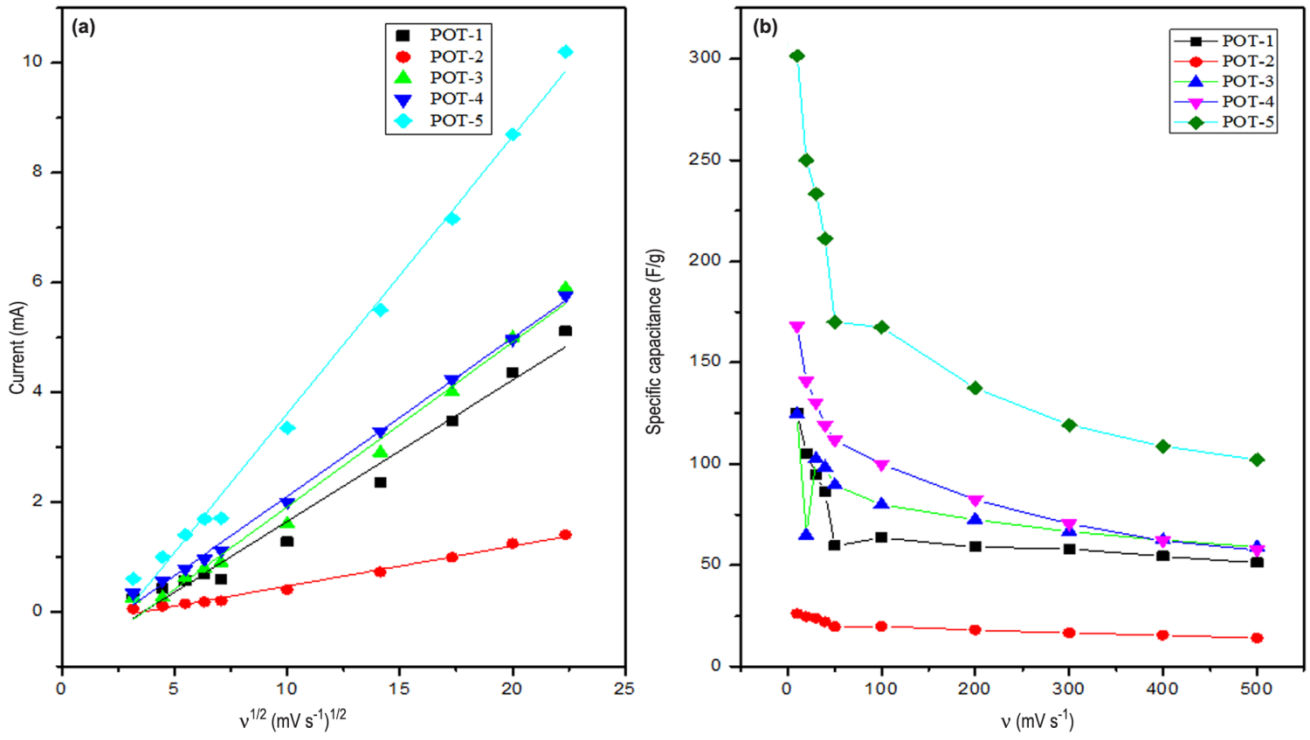

Fig. 2 – (a) First oxidation peak current versus square root of scan rate, and, (b) specific capacitance versus scan rate.

salts was carried out in potential window of 0 to 0.9 V. Charge discharge curves of POT are given in Fig. 3. At initial discharge, a sharp IR drop shows internal resistance of electrode material. The specific capacitance of electrode material[27-29] was calculated as $C = (I \times \Delta T)/ (\Delta \upsilon \times m)$, where "*I*", "$\Delta t$", "$\Delta V$" and "*m*" are the discharge current (A), discharge time (s), potential window (V) and mass of the active material, respectively[30]. As demonstrated in the charge-discharge characteristics, with decreasing the current, the discharge time increases (Fig. 3a & b). Electrolyte ions can approach the inner electrode material

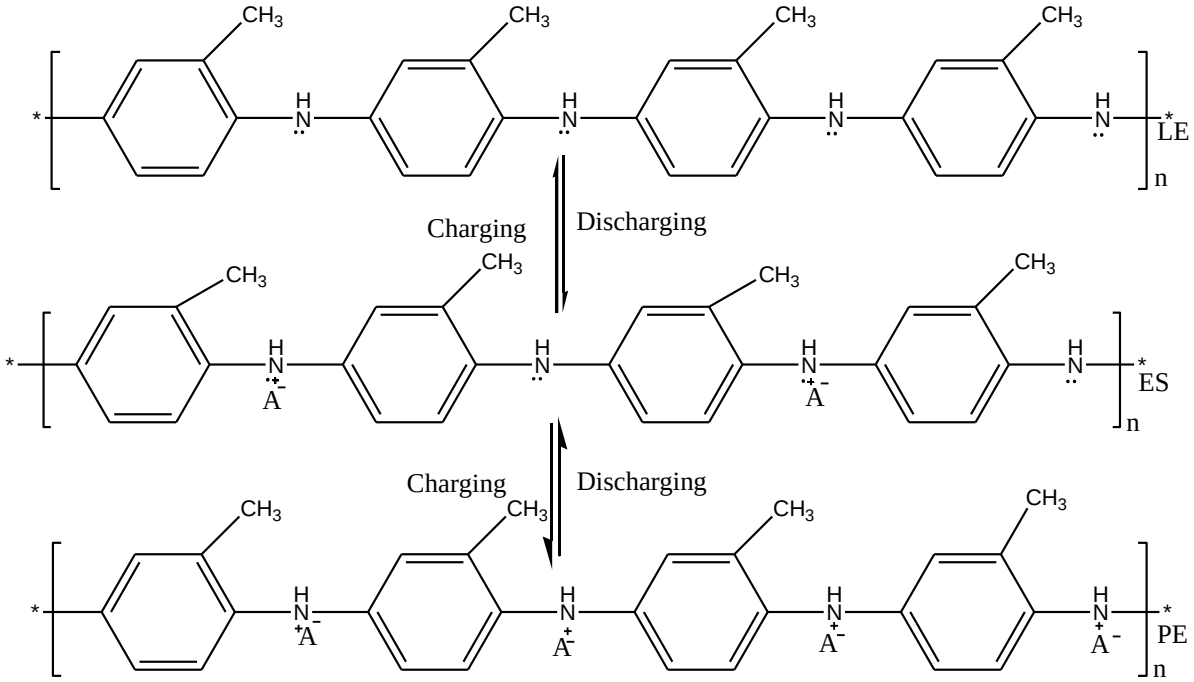

Charging and discharging in POT

Scheme 1

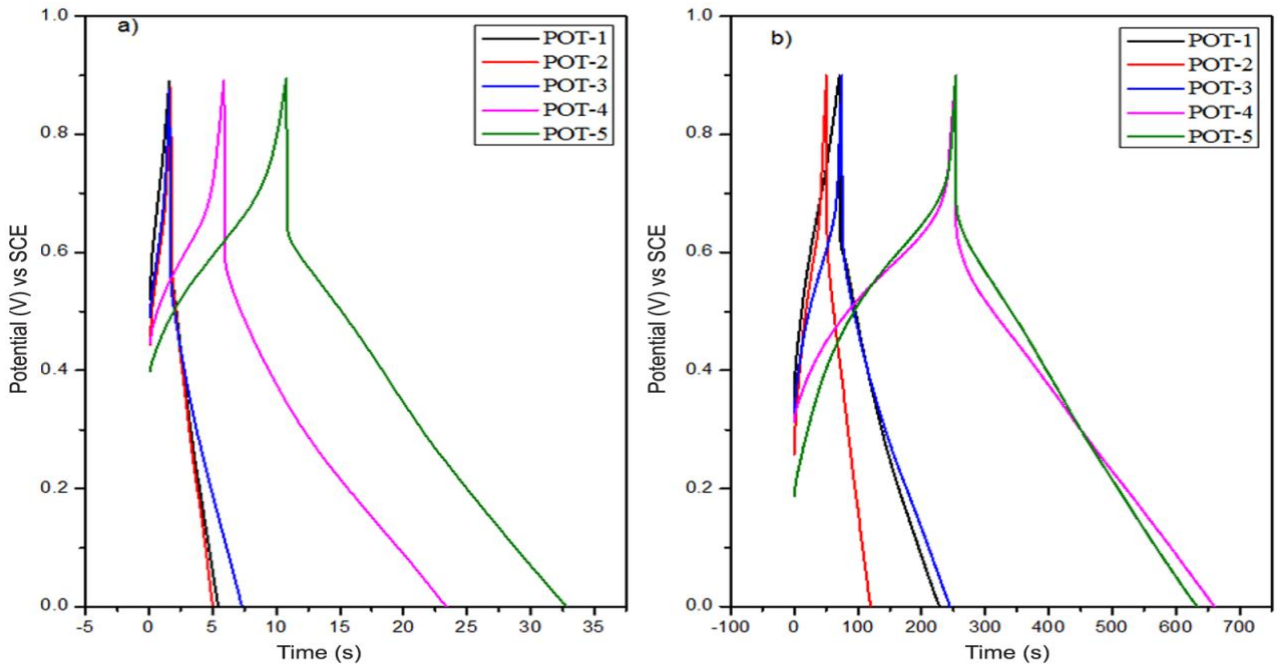

Fig. 3 – Galvanostatic charge discharge curves at (a) 5 A/g, and, (b) 0.5 A/g current density.

at lower current, which results in higher accessible surface and thus enhancing the specific capacitance. The lower capacitance at higher current density may be because of the shorter access time to the inner surface. It can further be noted that specific capacitance value calculated at discharge time at 5 A/g current density increases from POT-1 to POT-5. Once again POT-5 shows the highest specific capacitance value up to 122 F/g (Fig. 4) which is attributed to an increase in doping level and increased specific capacitance value, possibly due to the synergistic effect between POT chain and DBSA molecules[27]. However, at 0.5 A/g, discharge time increases from POT-1 to POT-4 and then decrease for POT-5 and thus highest specific capacitance value (226 F/g) was observed for POT-4 (Fig. 4). It is also noted that for all samples, specific capacitance value is lower at 5 A/g current density as compared to the value at 0.5 A/g. Indeed, efficient utility of active material is an important factor for pseudocapacitance of polymer materials[27].

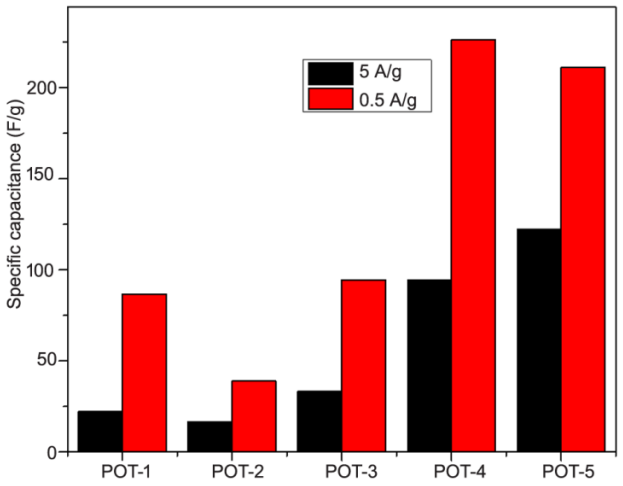

Fig. 4 – Specific capacitance of POT salts at 5 A/g and 0.5 A/g current densities.

The UV-visible spectra were registered in chloroform and are exhibited in Fig. 5a. Peaks observed at 250-308 nm are due to the л-л* transition of benzenoid rings[31]. Absorbance peak at 383-400 nm in the spectra of POT is because of the polaron-π* transition originating from quinoid ring[32]. The polymer in its doped form also shows band at 788-821 nm which arises due to the л-polaron transition[33]. It is clear from the spectra that all the POT samples were collected in the doped form. The extent of doping was calculated from $A_{788\text{-}821}/A_{250\text{-}308}$[15]. Table 1 shows that

Table 1 – The UV-vis absorption peaks of POT salts

Sample	Absorption peak wavelength (nm)			Extent of doping ($A_{788\text{-}821}/A_{259\text{-}308}$)
	π-π* transition	Polaron π* transition	Π-polaron transition	
POT-1	298	394	788	0.805
POT-2	259	399	814	0.88
POT-3	298	383	817	0.891
POT-4	302	384	821	1.125
POT-5	304	400	821	1.66

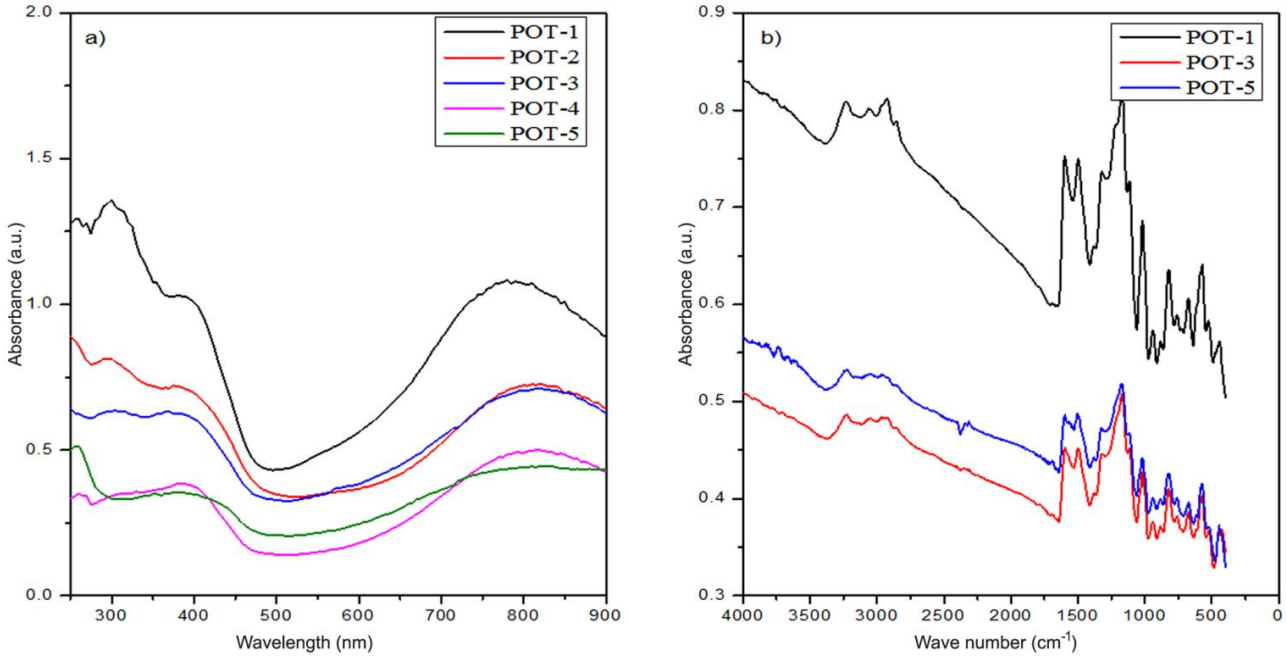

Fig. 5 – (a) UV-visible spectra POT salts in chloroform, and, (b) FTIR spectra of POT salts.

the doping level increases from POT-1 to POT-5; POT-5 shows the highest doping level up to 1.66. The trend is consistent with the CV and galvanostatic charge discharge data.

The key FTIR bands of POT-salts (Fig. 5b) are in good agreement with the IR frequencies of POT[34]. Strong bands corresponding to quinoid and benzenoid rings and the bands for dopant ions are present which clearly indicate the formation of conducting emeraldine salt phase of the polymer and supports FTIR and UV-visible spectroscopic results[34].

Two bands that are present in the vicinity of 1500 and 1600 cm^{-1} are assigned to the non-symmetric C_6 ring stretching mode. The higher frequencies vibration at 1600 cm^{-1} has a major contribution from the quinoid rings while the lower frequency contribution at 1500 cm^{-1} depicts the presence of benzoid ring unit. The presence of these two bands clearly shows that polymer is made up of amine and imine units[34].

The two bands attributed to S=O stretching mode of DBSA appear at ~671-678 cm^{-1} and ~1016-1022 cm^{-1} confirming the effective doping of POT by DBSA[35]. The presence of bands at ~3228-3234 cm^{-1} can be attributed to aromatic C-H stretching vibration[34]. The band at ~3048-3062 cm^{-1} is characteristic of C-H stretching due to substituted methyl group[33]. The characteristic bands at ~2924-2952 cm^{-1} may be assigned to aromatic C-H stretching vibration. Bands at ~2849-2855 cm^{-1} are due to the asssymetric $–CH_2-$ stretching of DBSA[35]. Bands for $(N-H)^+$ stretching vibration of unsaturated amines appear at ~2318-2339 cm^{-1}. Bands at ~1594-1601 cm^{-1} are due to C-N stretching of quinoid rings. The bands at ~1498 cm^{-1} are due to C-N stretching of benzoid rings[33]. Bands at ~1381-1387cm^{-1} are due to out-of-plane –CH bending of $–CH_3$ group[35]. For C-N stretching mode[31] the band appears at ~1319-1325 cm^{-1}. The bands at ~1160-1174 cm^{-1} are due to $–CH_3$ rocking of *o*-toluidine35. Bands at ~940-947 cm^{-1} are due to C-H stretching vibration of quiniod units. Bands for C-H deformation mode[31] appear at ~877-885 cm^{-1}. Bands that appear at ~822 cm^{-1} are due to pardistribution of aromatic rings indicating polymer formation. Bands at ~574-588 cm^{-1} are due to out of plane bending vibration. Vibration bands which are attributed to dopant ions and other peculiar bands are present, which verify that POT is present in conducting emeraldine salt form[33]. The two bands at ~1600-1608 cm^{-1} and ~1494-1502 cm^{-1} clearly show that the polymer is composed of amine and imine units, which gives further support to the earlier predictions that the polymer is composed of different oxidation states[15]. The intensity ratio of quinoid-to-benzenoid ring modes ($I_{\sim1600\text{-}1608}/I_{\sim1494\text{-}1502}$)[15] for POT-1, POT-3 and POT-5 are 1, 1 and 1.005 respectively.

When $I_{\sim1600\text{-}1608}/I_{\sim1494\text{-}1502}$) = 1.0, it corresponds to the polymer with higher conductivity and emeraldine-type structure. When level of oxidation of the polymer is increased beyond 1.0, conductivity is decreased[15]. When intensity ratio of quinoid-to-benzenoid ring modes ($I_{\sim1600\text{-}1608}/I_{\sim1494\text{-}1502}$) are compared, POT-5 displays the highest ratio of 1.005 as compared with that of POT-1 and POT-3. It can be presumed from the results given above that the production of the wholly oxidized pernigraniline form is somewhat more in POT-5. This is because of increased concentration of H_2SO_4 during synthesis, due to which oxidation of polymer chain occurs. As the quinoid-to-benzenoid ratio of POT-3 ($I_{\sim1600\text{-}1608}/I_{\sim1494\text{-}1502}$) (1.005) is very near to 1, the emeraldine salt form is dominant.

Crystallinity and orientation of conducting polymers are of much interest, because a highly ordered systems shows a metallic-like conductive state[36]. In Fig. 6, XRD patterns show that POT salts are semicrystalline in nature. Discrete sharp and intense peaks are observed in the diffraction patterns of POT salts. The sharp and highly intense peaks appear at $2\theta \approx 14^o, 16^o, 38^o, 44^o, 64^o$ while small peaks are observed at $2\theta \approx 24^o, 38^o, 57^o, 69^o$. Peak appearing at $2\theta \approx 24^o$ arises from the scattering perpendicular to the chain direction. Such a high crystallization may be due to substitution and H-bonding between sulfonic group on one ring and H on the ring of the adjacent chain =37. As shown in Fig. 6, with increase in H_2SO_4 concentration the crystallinity increases from POT 1 to POT 5 due to increasing doping level. With increase in doping level, crystallinity of POT salt increases. Such an effect can be explained by the fact that the insertions of doping anions between the polymer chains favor the crystalline state[15]. These results are in agreement with the UV-vis spectroscopy results illustrating that with increase in the amount of H_2SO_4 the doping level of POT increases. These results are also in agreement with literature, according to which nearly all conducting polymers have either amorphous or semicrystalline structure[38].

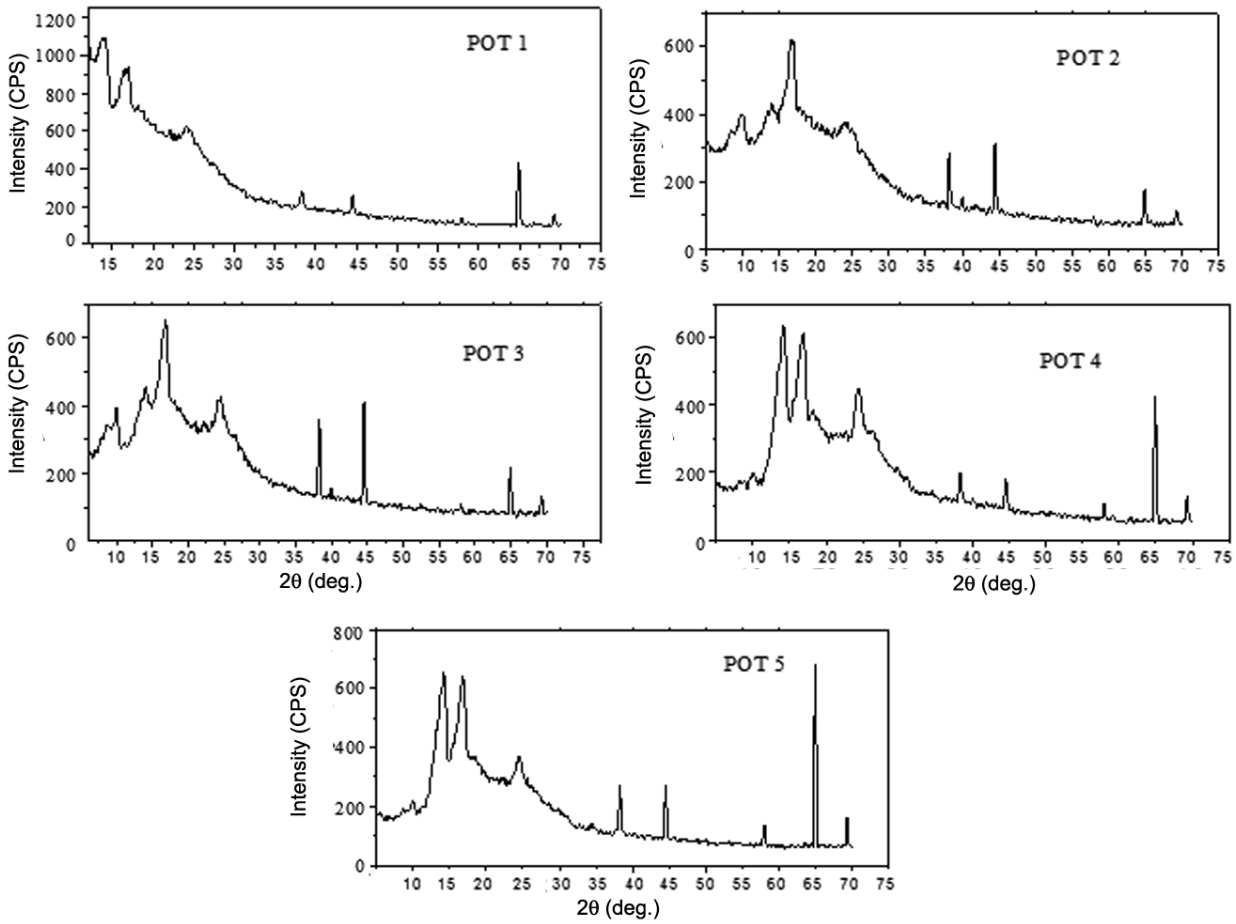

Fig. 6 – X-ray diffraction patterns of POT salts.

In the present study, POT-salt was utilized as a novel binder free low cost supercapacitor electrode material. At optimum conditions, the synthesized material showed a good specific capacitance of 301 F/g. Elimination of binder not only reduced the electrode processing cost but also improved the performance of electrode material. High electrochemical performance can be referred to the synergistic effect between POT and the dopant DBSA. The synthesized product displayed great application potential in supercapacitors or other power storage systems.

References

1 Zhang L L & Zhao X S, *Chem Soc Rev*, 38 (2009) 2520.
2 Van Hoa N, Quyen T T H, Van Hieu N, Ngoc T Q, Thinh P V, Dat P A & Nguyen H T T, *Synth Met*, 223 (2017) 192.
3 Pan C, Gu H & Dong L, *J Power Sources*, 303 (2016) 175.
4 Kahimbi H, Hong S B, Yang M & Choi B G, *J Electroanal Chem*, 786 (2017) 14.
5 Liu M, Shi M, Lu W, Zhu D, Li L & Gan L, *Chem Eng J*, 313 (2017) 518.
6 Jianhua L, Junwei A, Yecheng Z, Yuxiao M, Mengliu L, Mei Y & Songmei L, *ACS Appl Mater Interfaces*, 4 (2012) 2870.
7 Guan B, Li Y, Yin B, Liu K, Wang D, Zhang H & Cheng C, *Chem Eng J*, 308 (2017) 1165.
8 Kim T W & Park S J, *J Colloid Interface Sci*, 486 (2017) 287.
9 Zhang J, Gao J, Song Q, Guo Z, Chen A, Chen G & Zhou S, *Electrochim Acta*, 199 (2016) 70.
10 Li H, Wang J, Chu Q, Wang Z, Zhang F & Wang S, *J Power Sources*, 190 (2009) 578.
11 Wu Q, Xu Y, Yao Z, Liu A & Shi G, *ACS Nano*, 4 (2010) 1963.
12 Lindfors T & Latonen R M, *Carbon*, 69 (2014) 122.
13 Bilal S & Holze R, *J Electroanal Chem*, 592 (2006) 1.
14 Bilal S & Holze R, *J Electrochem Soc*, 155 (2008) 89.
15 Abdiryim T, Xiao G Z & Jamal R, *J Appl Polym Sci*, 96 (2005) 1630.
16 Fan L Z, Hu Y S, Maier J, Adelhelm P, Smarsly B & Antonietti M, *Adv Func Mater*, 17 (2007) 3083.
17 Bilal S, Gul H, Gul S & Shah A H A, *Iranian J of Sci Tech Trans A: Sci* (Accepted).
18 Wang H, Hao Q, Yang X, Lu L & Wang X, *ACS Appl Mater Interfaces*, 2 (2010) 821.
19 Bilal S, Farooq S & Holze R, *Synth Met*, 197 (2014) 144.
20 Bilal S & Holze R, *Electrochim Acta*, 54 (2009) 4851.
21 Jamal R, Abdiryim T & Nurulla I, *Polym Adv Technol*, 19 (2008) 1461.

22 Gupta V & Miura N, *Mater Lett*, 60 (2006) 1466.
23 Radhakrishnan S, Prakash S, Rao C R & Vijayan M, *Electrochem Solid-State Lett*, 12 (2009) 84.
24 Huang X, Hu N, Gao R, Yu Y, Wang Y, Yang Z, Kong E S W, Wei H & Zhang Y, *J Mater Chem*, 22 (2012) 22488.
25 Misoon O & Seok K, *Electrochim Acta*, 59 (2012) 196.
26 Radhakrishnan S, Muthukannan R, Kamatchi U, Rao C R K & Vijayan M, *Indian J Chem*, 50A (2011) 970.
27 Zhao Q, Chen J, Luo F, Shen L, Wang Y, Wu K & Lu M, *J Appl Polym Sci*, 134 (2017) 44808.
28 Tang L, Yang Z, Duan F & Chen M, *Colloids Surf A*, 520 (2017) 184.
29 Mitchell E, Candler J, De Souza F, Gupta R K, Gupta B K & Dong L F, *Synth Met*, 199 (2015) 214.
30 Lei D, Song K H, Li X D, Kim H Y & Kim B S, *J Mater Sci*, 52 (2017) 2158.
31 Abdiryim T, Xiao-Gang Z & Jamal R, *J Appl Polym Sci*, 96 (2005) 1630.
32 Mucuk Z, Karakışla M & Saçak M, *Int J Polym Anal Charact*, 14 (2009) 403.
33 Kulkarni M V, Kasi Viswanath A & Khanna P K, *J Macromol Sci Pure Appl Chem*, 43 (2006) 197.
34 Kulkarni M V & Viswanath A K, *Eur Polym J*, 40 (2004) 379.
35 Shreepathi S & Holze R, *Macromol Chem Phys*, 208 (2007) 609.
36 Kumari K, Ali V, Rani G, Kumar S, Lakshmi G B V S & Zulfequar M, *Mater Sci Appl*, 2 (2011) 1049.
37 Ebrahim S M, Gad A & Morsy A, *Synth Met*, 160 (2010) 2658.
38 Kumar A, Ali V, Kumar S & Husain M, *Int J Polym Anal Charact*, 16 (2011) 298.